

Figure 3. Pre- and post-flood map (2017).

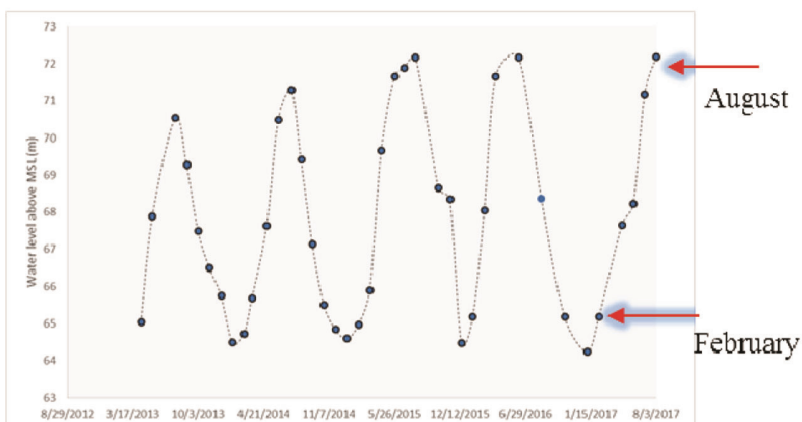


Figure 4. Water-level variation of Brahmaputra river in KNP.

exemplified flooding season. Sentinel 1A is a polar orbiting day-and-night satellite that works in the C-band range. Therefore, Sentinel dataset is most suitable to

assess flooding condition, specifically under cloud-cover condition.

The flood situation in Assam became very critical during the second week of

August 2017, affecting several districts of the state. Flood has affected the expanse of the Brahmaputra river, which has increased by 3–5 times in some parts during this period (February to August 2017; Figure 3). Around 67% of grassland was inundated on 12 August 2017 (Figures 2 and 3). SARAL/AltiKa data were processed using the ICE-1 retracking method. The water-level variation provides information about the status of inundation of the flooded area<sup>3</sup>. The water level increased by ~7 m from February to August 2017 (Figure 4).

The present study has successfully demonstrated the use of freely available data for a quick assessment of the recent flood of 2017 affecting KNP. A detailed study can be done to assess the flood vulnerability of KNP, specifically considering the ecological importance of this Park.

- CWC and NRSC. (2014, March); <http://www.india-wris.nrsc.gov.in/Publications/BasinReports/Brahmaputra%20Basin.pdf> (last accessed on 21 August 2017).
- Kushwaha, S. P. S. et al., Project report, IIRS/FED/Kaziranga/36/8026/2008.
- Ghosh, S., Nandy, S. and Senthil Kumar, A., *Curr. Sci.*, 2016, **111**(9), 1450–1451.

Received 28 August 2017; revised accepted 14 June 2018

SURAJIT GHOSH\*  
RAJ KUMAR  
UTTARA PANDEY  
PARUL SRIVASTAVA  
SWAPAN MEHRA

IORA Ecological Solutions Pvt Ltd,  
225B, FF, Indraprastha,  
Gyanamandir Complex,  
Lado Sarai Village,  
New Delhi 110 030, India

\*For correspondence.  
e-mail: surajitghosh.ind@gmail.com

## Non-tectonic signals in tectonic geodesy

Earth's gravitational field, its shape and orientation in the space are the 'three pillars of geodesy'<sup>1,2</sup>. In recent times, geodesy has emerged as an interdisciplinary domain in geophysics, which includes

tectonics, internal structure of the earth, seismology, hydrology, glaciology, oceanography, meteorology, atmospheric physics, climate science, etc.<sup>1</sup>. In fact, it has found several applications in earth

sciences that a new subject 'tectonic geodesy' has evolved, which specifically deals with the application of geodetic techniques in understanding tectonic processes by estimating surface velocity

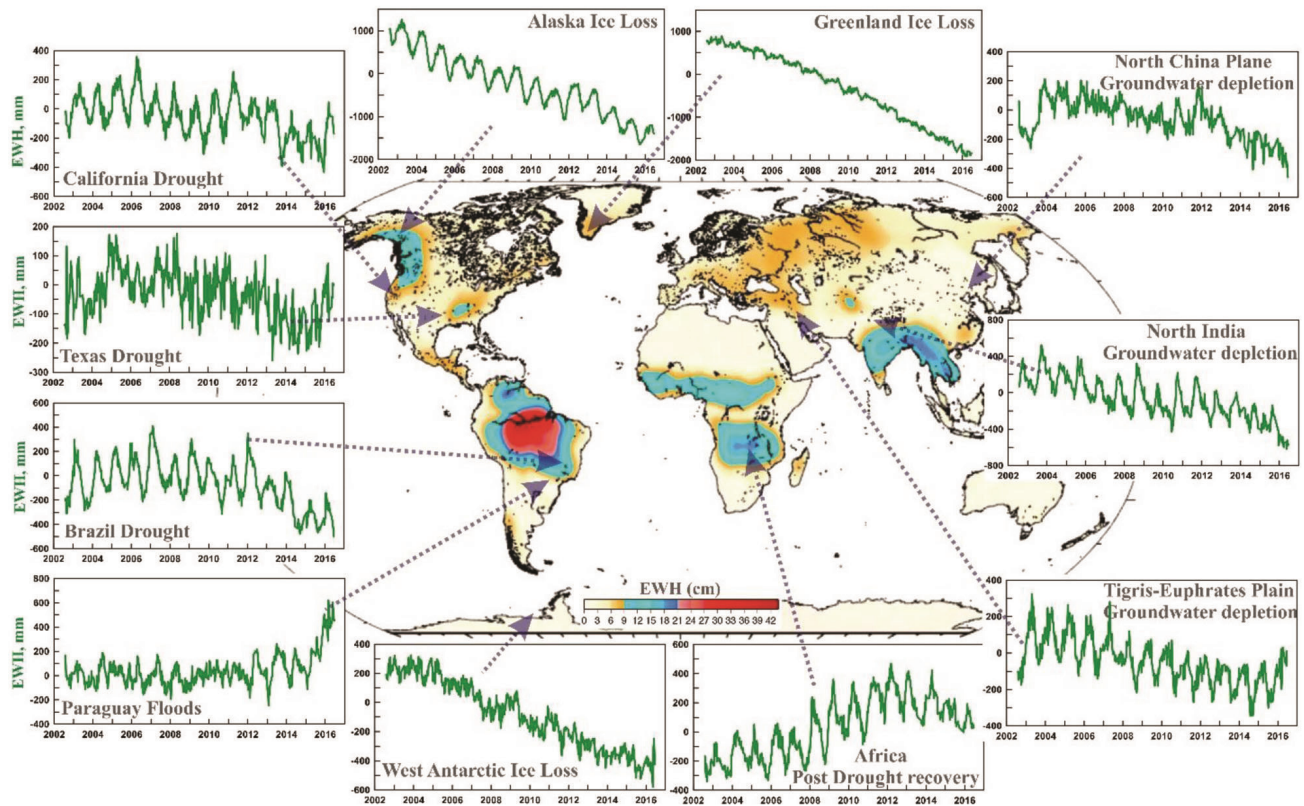


**Figure 1.** Global trend signals in 15 years of GRACE data from April 2002 to June 2017, illustrating mass change due to changes in total terrestrial water storage (TWS; mm). Background image shows global peak-to-peak equivalent water height (EWH; cm) measured from GRACE (modified from Fu *et al.*<sup>4</sup>).

field within tectonically active regions. This technique provides constraints on the spatio-temporal distribution of the lithospheric deformation and surface plate kinematics by exploiting various space-based geodetic techniques (e.g. Global Positioning System (GPS), Very Long Baseline Interferometry (VLBI), Interferometric Synthetic Aperture Radar (InSAR), Doppler Orbitography and Radio positioning Integrated by Satellite (DORIS) and Satellite Laser Ranging (SLR)).

Further, since the launch of two twin satellites of the Gravity Recovery and Climate Experiment (GRACE) during the mission in 2002 (ref. 3), spatio-temporal variations in the earth's gravity field due to mass variation can be quantified. Using this robust technique, we can characterize earth's time-varying gravity field, decade-scale mass change and mass redistribution trend due to variation in the hydrological cycle, seasonal hydrological effects, ice-mass loss of glaciers and ice sheets, sea-level changes, flood and drought potential, substantial

depletion of groundwater storage from aquifers, etc.<sup>5–10</sup>. Taking advantage of continuous Global Positioning System (cGPS) measurements and satellite gravimetric data from GRACE, we are now able to tease out the 'non-tectonic' signals by analysing continental water storage, its spatio-temporal evolution and ground subsidence rate which are beyond the conventional trends of 'tectonic geodesy'.

The past 15 years of satellite gravimetric data (from GRACE) since April 2002, have witnessed more than decadal-scale global mass change and redistribution process, in terms of changes in the total terrestrial water storage (TWS) due to various non-tectonic processes (Figure 1). It is also complemented by the cGPS observations which register well the loading (unloading) non-tectonic deformation signals (Figure 2). Here we present only a few but representative global case histories. For example, regions in the North China Plain (China), Indo-Ganga Plain (India), and Tigris-Euphrates Plain (Iran, Turkey) are experiencing abnormal ground subsidence and substantial lowering of total TWS due to extensive pumping of groundwater from the aquifers in response to the growing demand, irrigation and urbanization (Figure 3, top panel). Unfortunately, it does not end there. Now, it has been reported that although natural faulting itself is a tectonically driven phenomenon, such anthropogenic crustal unloading due to extensive groundwater pumping can also modify subsurface stress and influence seismic activity<sup>11–14</sup>. On the other hand, global-scale seasonal mass movement causes periodic crustal deformation (e.g. seasonal rainfall-induced deformation in Southeast Asia, the Amazon Basin, snow-induced periodic crustal loading in Alaska and Japan<sup>4,6,15,16</sup>), which can also be quantified through combined analysis of GRACE and cGPS data. It has been observed that in case of normal precipitation cycle, the annual precipitation equals the evaporation and surface run-off and thus the resulting seasonal loading is balanced by the unloading process (i.e. subsidence is

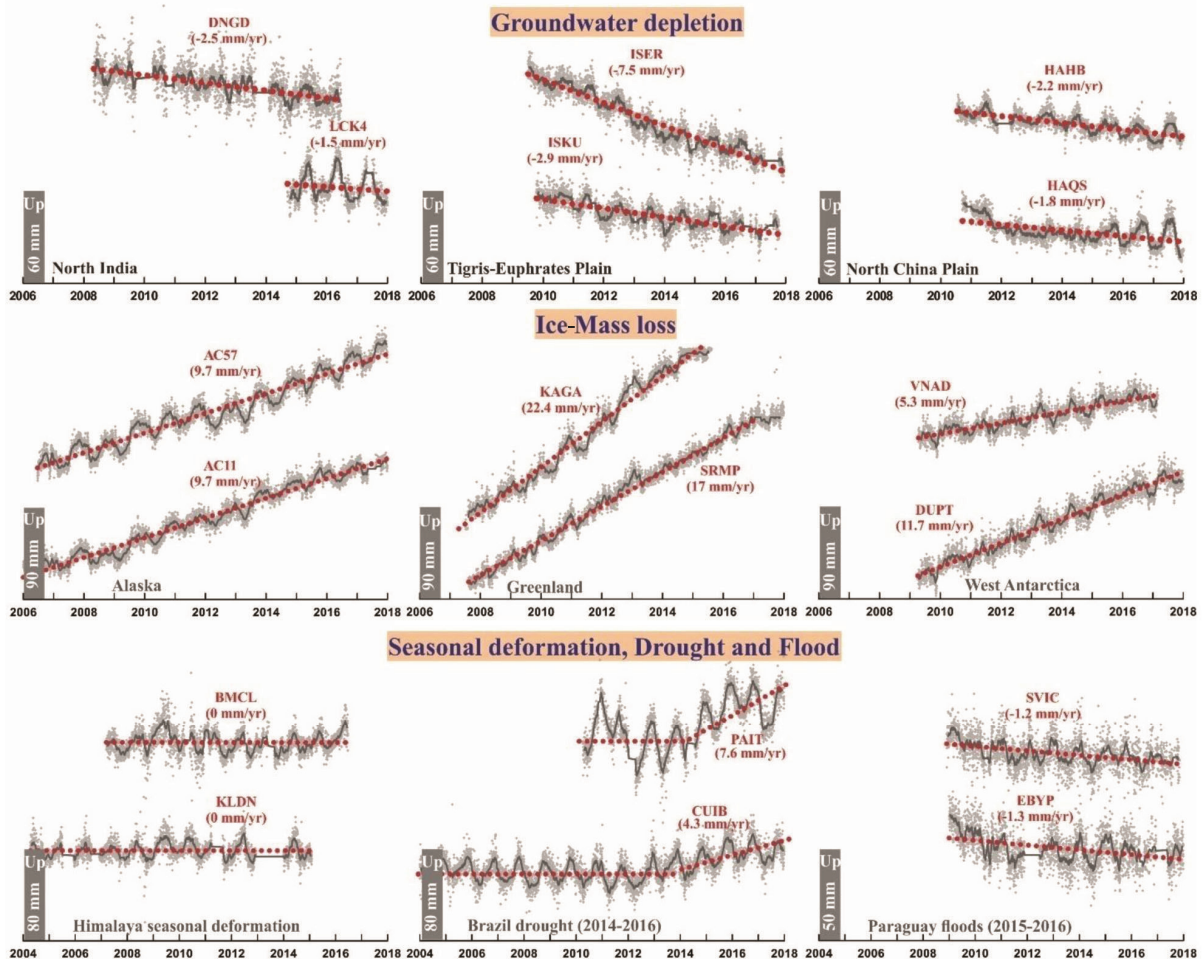


**Figure 2.** Evidences from cGPS-derived vertical displacement (globally), showing representative scenarios for groundwater depletion, ice-mass loss, seasonal deformation, and drought and flood situation.

balanced by the uplift). In such cases, long-term trend in TWS in GRACE and in vertical component of cGPS time series, appears as neutral or exhibits zero trend (Figure 3, middle panel – black curve). However, during drought and flood periods such balance is disturbed. During severe drought period, annual precipitation is generally less than the evaporation and surface run-off, and the resulting seasonal loading is less than the unloading; so there is a net uplift (Figure 3, middle panel – orange curve). The situation is reversed during flooding period, which results in net subsidence (Figure 3, middle panel – green curve). In this context normal seasonal deformation in the Himalaya, California drought (2011–15), Texas drought (2011–15), Brazil drought (2014–16), post-drought recovery in Africa (post 2007) and Paraguay floods (2013–15) are ideal examples to cite for such variations in seasonal loading and associated crustal movements (Figures 1

and 2). Finally, the interior of the earth responds to changes in surface load due to the retreat and advance of ice sheets, through viscoelastic deformation seeking to gain a new equilibrium state. This glacial isostatic adjustment induces changes in the earth's gravity field, rotation of the earth, surface geometry and sea-level height<sup>3</sup>. Ice-mass loss from west Antarctica, Greenland and Alaska, and subsequent uplift of the lithosphere by upward mantle flow through viscoelastic deformation are ideal examples for that aspect (Figure 3, lower panel).

Using GRACE-derived hydrological model, several previous works have modelled seasonal displacement (i.e. north, east and vertical) captured by cGPS time series<sup>4,5,17</sup>. However, in a number of cases a disagreement between GPS-measured and GRACE (and hydrological)-modelled seasonal deformation has been reported. Fu *et al.*<sup>4</sup> argued that this might be due to low spatial resolution

of GRACE, spatial smearing and some local effects, such as groundwater extraction, irrigation process, etc. Chanard *et al.*<sup>17</sup> have attributed it to earth structure and geocentre motion. Gautam *et al.*<sup>18</sup>, who addressed the concerns of Chanard *et al.*<sup>17</sup>, reported it to be due to low resolution of the hydrological models derived from GRACE data. Gahalaut *et al.*<sup>19</sup> argued that impoundment of reservoir and its water-level fluctuation can also affect the cGPS time series in a complicated manner. However, such local effects cannot be captured in GRACE data due to its poor resolution. Despite the above inherent difficulties, a combination of cGPS and GRACE measurements addresses non-tectonic processes spanning from few days to few decades. Hopefully, the resolution of hydrological models would improve in future, either by incorporating satellite- or land-based observations which would facilitate in teasing out these, although non-tectonic, yet

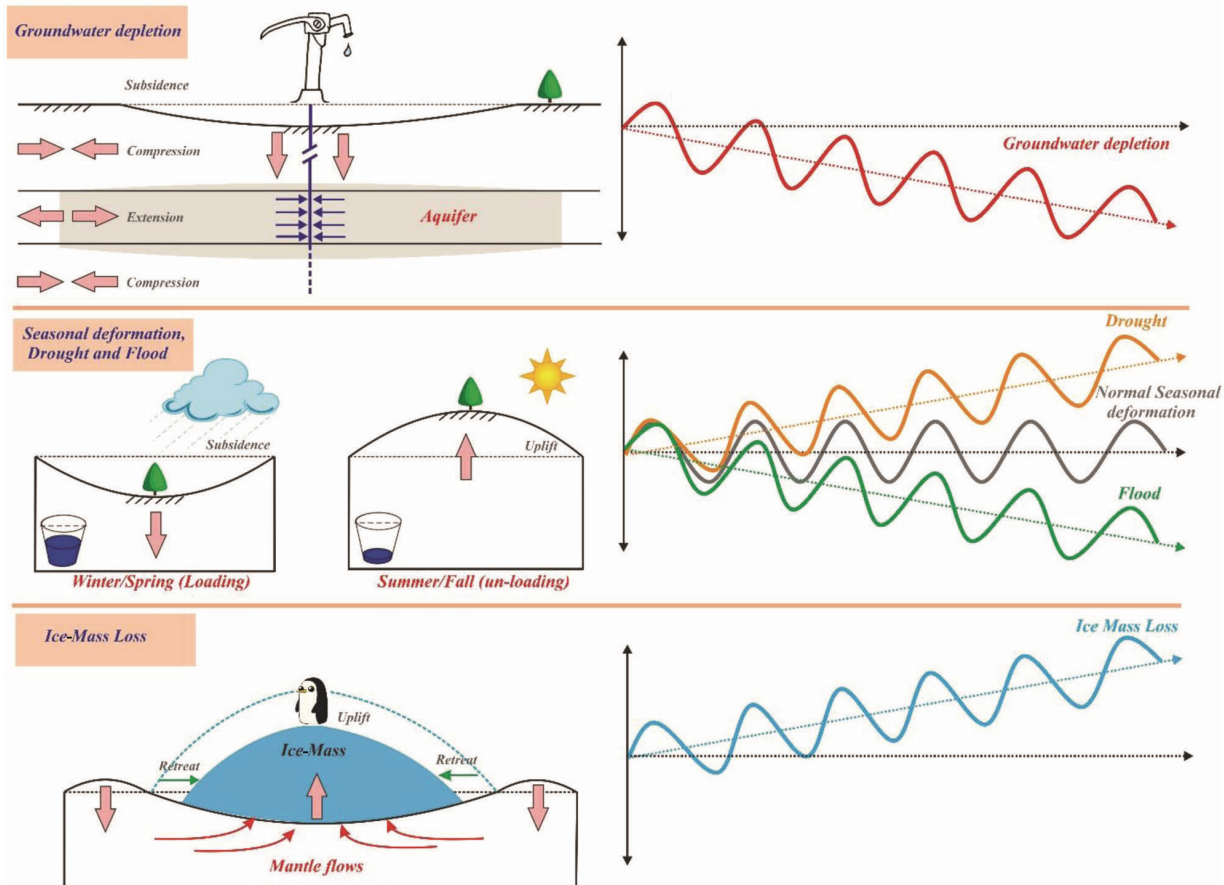


**Figure 3.** Schematic interpretation and effect on cGPS displacement (vertical) time series for groundwater depletion, normal seasonal deformation, drought and flood situation, and ice-mass loss.

important response of various shallow surface or subsurface processes. This non-tectonic signals need to be identified and taken into account to improve our understanding of tectonic processes, which also operate on the same or even larger timescale.

1. Beutler, G. *et al.*, *J. Geodesy*, 2004, **77**, 560–575.
2. Blewitt, G., *Treatise on Geophysics*, Elsevier, Oxford, 2015, vol. 3, 307–338.
3. Wouters, B. *et al.*, *Rep. Prog. Phys.*, 2014, **77**, 116801.
4. Fu, Y. *et al.*, *Geophys. Res. Solid Earth*, 2013, **40**, 6048–6053.
5. Bettinelli, P. *et al.*, *Earth Planet. Sci. Lett.*, 2008, **266**, 332–344.
6. Fu, Y. *et al.*, *Geophys. Res. Lett.*, 2012, **39**, L15310.
7. Chen, J. *et al.*, *J. Geophys. Res.*, 2010, **115**, D22108.
8. Khan, S. A. *et al.*, *Geophys. Res. Lett.*, 2010, **37**, L06501.
9. Voss, K. A. *et al.*, *Water Resour. Res.*, 2013, **49**, 904–914.

10. Borassa, A. A. *et al.*, *Sci. Expr.*, 2014, **345**, 1587–1590.
11. Foulger, G. R. *et al.*, *Earth Sci. Rev.*, 2017, **178**, 438–514.
12. Kundu, B. *et al.*, *Geophys. Res. Lett.*, 2015, **42**, 10607–10613.
13. Amos, C. B. *et al.*, *Nature*, 2014, **509**, 483–486.
14. González, P. J. *et al.*, *Nature Geosci.*, 2012, **5**, 821–825.
15. Fu, Y. and Freymueller, J. T., *J. Geophys. Res.*, 2012, **117**, B03407.
16. Heki, K., *Earth Planet. Sci. Lett.*, 2003, **207**, 159–164.
17. Chanard, K. *et al.*, *J. Geophys. Res.*, 2014, **119**, 5097–5113.
18. Gautam, P. K. *et al.*, *Quaternary Int.*, 2017, **462**, 124–129.
19. Gahalaut, V. K. *et al.*, *Geophys. J. Int.*, 2017, **209**, 425–433.

**ACKNOWLEDGEMENTS.** For seasonal deformation model, we used 10-day solutions of GRACE data archived from the Centre National d'Etudes Spatiales/Groupe de Recherche de Géodésie Spatiale (CNES/GRGS), available at <http://grgs.obs-mip.fr/>. GPS time-

series data used here can be accessed at <http://geodesy.unr.edu/NGLStationPages/gpsnetmap/GPSNetMap.html>. Equivalent water height was computed using hydrological modelling software package, which can be accessed at <http://web.gps.caltech.edu/~avouac/software.html>. D.P. is supported by NITR Research Fellowship. We thank an anonymous reviewer for constructive comments.

Received 5 February 2018; revised accepted 26 June 2018

BHASKAR KUNDU<sup>1,\*</sup>  
DIBYASHAKTI PANDA<sup>1</sup>  
VINEET K. GAHALAUT<sup>2</sup>

<sup>1</sup>Department of Earth and Atmospheric Sciences,  
NIT Rourkela, Rourkela 769 008, India

<sup>2</sup>National Centre for Seismology,  
Ministry of Earth Sciences,  
New Delhi 110 003, India

\*For correspondence.  
e-mail: rilbhaskar@gmail.com